31P and195Pt solid-state NMR and DFT studies on platinum(i) and platinum(II) complexes

Journal Name

ARTICLE

^{31}P and ^{195}Pt Solid-State NMR and DFT Studies on Platinum(I) and Platinum(II) Complexes

Received 00th January 20xx,
Accepted 00th January 20xx

DOI: 10.1039/x0xx00000x

www.rsc.org/

Stefano Todisco[a], Giacomo Saielli[b], Vito Gallo[a], Mario Latronico[a], Antonino Rizzuti[a], Piero Mastrorilli*[a]

^{31}P and ^{195}Pt solid state NMR spectra on *anti*-[(PHCy)ClPt(μ-PCy$_2$)$_2$Pt[(PHCy)Cl] (**3**) and [(PHCy$_2$)Pt(μ-PCy$_2$)(κ^2*P,O*-μ-POCy$_2$)Pt(PHCy$_2$)] (*Pt-Pt*) (**4**) were recorded under cross polarization/magic-angle spinning conditions (^{31}P) or with the cross polarization/Carr-Purcell Meiboom-Gill pulse sequence (^{195}Pt) and compared to data obtained by relativistic DFT calculations of ^{31}P and ^{195}Pt CS tensors and isotropic shielding at the ZORA Spin Orbit level. A good agreement with experimental results was found and it was possible to rationalize the chemical shift differences of ^{195}Pt and ^{31}P nuclei between compounds **3** and **4** as mostly due to a change (in opposite directions for ^{195}Pt and ^{31}P) of the principal component of the shielding tensor perpendicular to the molecular plane defined by the Pt and P atoms. Paramagnetic and spin-orbit terms were found the most important contributions to ^{195}Pt and ^{31}P shielding.

Introduction

Solid state NMR acts as a bridge between structural XRD information and solution NMR spectra.[1] As part of our studies on phosphanido bridged platinum complexes[2] we became interested to the factors influencing ^{31}P and ^{195}Pt NMR features of these complexes, and we reported that structural parameters (the presence or absence of Pt–Pt bond, for instance) rather than the formal oxidation state of the metal, play a major role in determining the isotropic ^{31}P and ^{195}Pt chemical shifts.[3] Chart I shows the ranges of ^{31}P and ^{195}Pt chemical shifts for diorganophosphanido platinum complexes. It is apparent that molecules characterised by the presence of *four*-membered P$_2$Pt$_2$ rings (*not* displaying any Pt–Pt bond) show relatively deshielded ^{195}Pt nuclei (δ_{Pt} from –2000 to –4000) and relatively shielded ^{13}P nuclei (δ_P from 0 to –270) when compared to molecules characterised by *three*-membered PPt$_2$ rings (thus displaying a Pt–Pt bond) which show relatively shielded ^{195}Pt nuclei (δ_{Pt} from –4800 to –7000) and relatively deshielded ^{13}P nuclei (δ_P from +400 to +80).
In this framework, we have recently demonstrated that the strong difference in NMR chemichal shift displayed by ^{31}P and ^{195}Pt nuclei, comparing the dinuclear phosphanido-bridged complexes **1** and **2** (Chart II), [complexes **1** and **2** differ only for the Pt oxidation states, +2 for **1** and +3 for **2**, and for the geometry of the Pt$_2$P$_2$ core] is caused mainly by one of the three principal components of the chemical shift (CS) tensor.[3]

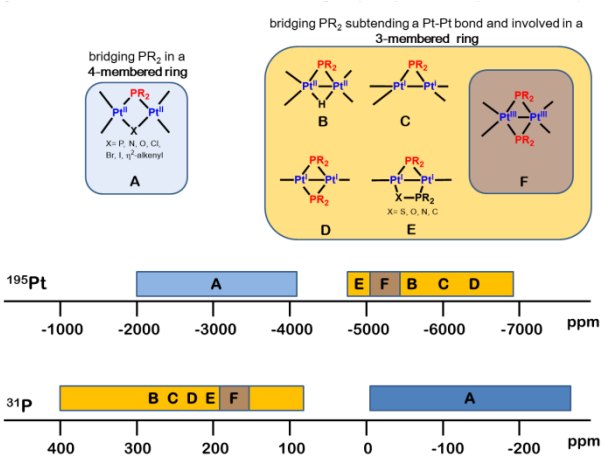

Chart I Ranges of ^{31}P and ^{195}Pt chemical shifts for diorganophosphanido platinum complexes.

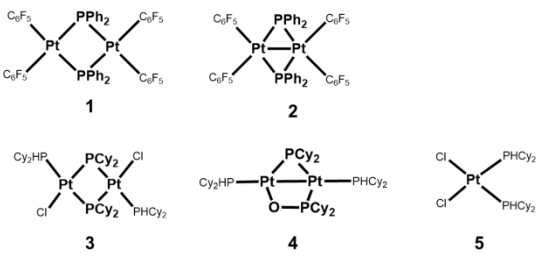

Chart II Phosphanido bridged diplatinum complexes.

[a] Dipartimento di Ingegneria Civile, Ambientale, del Territorio, Edile e di Chimica (DICATECh), Politecnico di Bari, via Orabona 4, I-70125 Bari, Italy.
[b] Istituto per la Tecnologia delle Membrane, Unità di Padova CNR, via Marzolo, 1 - 35131, Padova, Italy.

Journal Name

ARTICLE

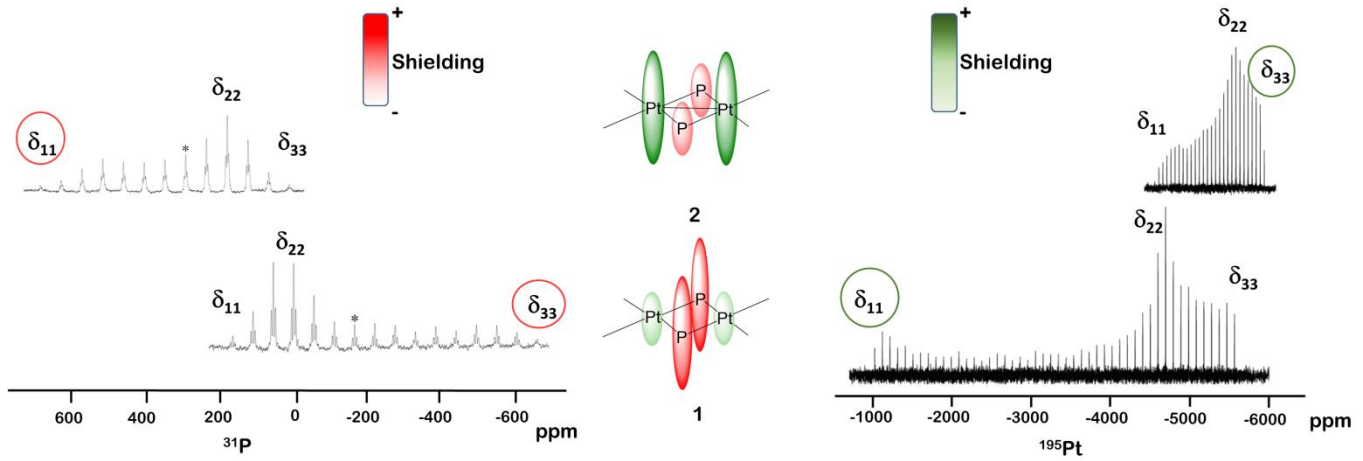

Fig. 1 ^{1}H-^{31}P CP/MAS (left) and static ^{1}H-^{195}Pt CP/CPMG (right) NMR spectra of **1** and **2**.[3] The distinct principal components (^{31}P: δ_{11} for **2** and δ_{33} for **1;** ^{195}Pt: δ_{11} for **1** and δ_{33} for **2**) are in all cases oriented along the direction perpendicular to the Pt_2P_2 plane. Orientation and magnitude of the distinct components of the CS tensors for ^{31}P and ^{195}Pt nuclei in complexes **1** and **2** are also shown. The presence of the Pt-Pt bond, in these otherwise identical structures, brings about a dramatic change of nuclei shielding.

Figure 1 shows the powder pattern of the ^{1}H-^{31}P CP/MAS NMR spectrum of **1** and **2** from which is apparent that the magnitude of one component of the CS tensor varies by ca 1350 ppm, with the other two components remaining constant. The same behaviour was observed by studying the powder pattern of the solid state ^{195}Pt NMR spectrum of **1** and **2** (Figure 1) in which only one of the the three components of the CS tensor strongly varies (by ca. 5000 ppm).

DFT calculations permitted to determine the orientation of the principal components of the CS tensors, pointing out that, for both complexes **1** and **2**, the distinct component is the one oriented along the direction perpendicular to the Pt_2P_2 plane (Figure 1). Moreover, the main contribution to the distinct component of the CS tensor was found to stem mainly from the paramagnetic term (σ_p) for both ^{195}Pt and ^{31}P,[3] thus pointing out a key role of the molecular orbital energies of the molecules for the values of the distinct component of the CS tensors.

Since the only difference between complexes **1** and **2** is the valence electron count (VEC), it is conceivable that a limited number of MO is accountable for the values of the distinct components of the CS tensors, including, in the case of **2**, the MO responsible for the Pt–Pt bond. This hypothesis seems supported by the circumstance that isotropic ^{31}P and ^{195}Pt NMR chemical shifts of phosphanido-bridged dinuclear Pt(I) complexes, in which a Pt-Pt bond is invariably present, fall in the same CS region of the Pt(III) systems (Chart I).

Intrigued by these considerations, we decided to carry out an experimental study on ^{31}P and ^{195}Pt NMR in the solid state of two related dinuclear Pt complexes in which the formal oxidation states of Pt are +2 and +1 with the aim of gaining insights into the origin of the chemical shift (geometry, Pt oxidation state) and its relationships to electronic structures. The experimental data have been compared with the results of relativistic DFT calculations, at the Spin-Orbit level, of single molecules in vacuo (thus neglecting specific solid-state effects on the NMR properties).

Relativistic DFT, in particular the inclusion of spin-orbit effects, has proven to be very effective at predicting NMR properties of heavy atoms.[4] Recent applications include halogenated natural products,[5] ^{129}Xe NMR in ionic liquids[6] and metallated cryptophanes,[7] metallasilatrane[8] and metal-based catalysts.[9] Analysis of solid state systems and tensorial components have also been successfully reported using single molecule calculations[3]: although the perturbations of the periodic lattice on the NMR properties might be relevant in case of inorganic salts[10], we expect such effects to be much less important in molecular solids.

The complexes chosen for this combined solid state NMR and DFT study are the Pt^{II}–Pt^{II} species *anti*-[(PHCy)ClPt(μ-PCy_2)$_2$Pt(PHCy)Cl] (**3**, Chart II), and the Pt^{I}–Pt^{I} complex [$(PHCy_2)$Pt(μ-PCy_2)(κ^2*P,O*-μ-$POCy_2$)Pt($PHCy_2$)] (*Pt-Pt*) (**4**, Chart II). The work has been completed with the mononuclear species *cis*-$PtCl_2(PHCy_2)_2$ (**5**, Chart II), in which the Pt atom bears ligands present in **3** (Cl and $PHCy_2$) but does not possess any bridging phosphanido group.

Results and discussion

^{1}H-^{31}P CP/MAS NMR

The ^{1}H-^{31}P CP/MAS spectrum of the Pt(II) complex **3** is shown in Figure 2, with the ^{31}P NMR parameters reported in Table 1. Recording the spectrum at different spinning rates (11.0 and 15.0 kHz) permitted to assign the isotropic ^{31}P chemical shifts which were found at δ –142.6 (phosphanide) and δ 16.9 (phosphane), in good agreement to the values found in $CDCl_3$ solution (δ –137.9 and δ 15.1, respectively).[11] Each signal is flanked by ^{195}Pt satellites from which the indirect coupling constants of 1960 Hz (^{1}JP^{2}-Pt) and ca. 2312 Hz (average of ^{1}JP^{1}-Pt^{1} and ^{1}JP^{1}-Pt^{2}) could be extracted (the corresponding values for the spectrum in solution are: ^{1}JP^{2}-Pt =1948 Hz; ^{1}JP^{1}-Pt^{1} = 2048 Hz and ^{1}JP^{1}-Pt^{2} = 2399 Hz).[11] The isotropic ^{31}P signal of the coordinated $PHCy_2$ shows an apparent doublet, the separation of which (363 Hz) corresponds to the sum of J_{AX}+$J_{AX'}$ (366.5 Hz in solution[11]).

The anisotropy of the bridging phosphanide ^{31}P is quite larger than that of the terminal phosphane, as measured by the span Ω of the chemical shift (CS) tensor that is 758 ppm for μ-PCy and 152 ppm for $PHCy_2$. For the related complex *anti*-[$(PH_2Mes)ClPt(\mu\text{-}PHMes)_2Pt(PH_2Mes)Cl$] (**6**) (Mes = 2,4,6-$Me_3C_6H_2$) reported by Glueck et al., the span Ω values for the ^{31}P signals of μ-PHMes and PH_2Mes are 712 ppm and 85 ppm, respectively.[12] The only other phosphanido bridged platinum complex for which are available the solid-state NMR parameters is complex **1**, showing a Ω of 840 ppm.[3] Another common feature to complexes **3** and **1** is the positive value of the skew κ, 0.82 for **3** and 0.80 for **1**. Although no HB analysis has been reported for **6**, the appearance of the ^{31}P signal of μ-PHMes clearly indicates a positive value of the skew (the distinct principal component is δ_{33} and falls at about –700 ppm).

The ^{1}H-^{31}P CP/MAS spectrum of the Pt(I) complex **4** featuring a Pt–Pt bond is shown in Figure 3.

Complex **4** contains four different ^{31}P atoms belonging to a bridging phosphanide, two phosphanes and a phosphinite. The presence of ^{195}Pt satellites for each ^{31}P signal hampered the HB analysis, so only the isotropic chemical shifts and the indirect coupling constant $^{1}J_{P,Pt}$. could be obtained from the spectrum (Table 1). The chemical shifts found in the solid state (P^{1}, δ 133.2, $^{1}J_{P,Pt2}$ = 3096 Hz, $^{1}J_{P,Pt1}$ = 3969 Hz; P^{2}, δ 23.7, $^{1}J_{P,Pt1}$ = 4278 Hz; P^{3}, δ 97.3, $^{1}J_{P,Pt2}$ = 3066 Hz; P^{4}, δ 15.6, $^{1}J_{P,Pt2}$ = 3668 Hz) are comparable to those observed in C_6D_6 solution.[11]

Examination of the ^{31}P phosphanido peaks in Figure 3 reveals that spinning at 9.0 kHz was sufficient to break down all spinning side bands except the first ones. Comparison of the features of **4** with those of **2**, two complexes having both a VEC of 30 and a Pt–Pt bond, reveals that the presence of the four-membered Pt-O-P-Pt ring fused with the three membered Pt-μ-P-Pt ring results in a significantly smaller value of Ω for **4**, that is reflected in a different isotropic chemical shift of the phosphanide (for **4** δ_{P1} = 133.2; for **2** δ_{P1} = 292). This effect, albeit empirical at this stage, seems confirmed by the isotropic ^{31}P chemical shifts of the phosphanido-Pt complexes depicted in Chart III, where such values go from $\delta_{\mu\text{-}P}$ = 133.2 for **4** (and $\delta_{\mu\text{-}P}$ = 140.3 for the sulfur analogue **7**[13]) to $\delta_{\mu\text{-}P}$ = 196.4 for **8**[2f] and $\delta_{\mu\text{-}P}$ = 183.6 for **9**.[13]

The ^{1}H-^{31}P CP/MAS spectrum of **5** (Figure 4) shows two different signals at δ 7.8 and δ –4.9, integrated 1:1, indicating the presence of two crystallographically inequivalent phosphorus nuclei within the molecule, a circumstance already observed for the related complexes *cis*-$PtCl_2(PMePh_2)_2$, *cis*-$PtCl_2(PPh_3)_2$,[14] *cis*-$PtCl_2(PMePh_2)_2$, *cis*-$PtCl_2\{PPh(CH{=}CH_2)_2$,[15] and *cis*-$PtCl_2(PEt_3)_2$,[16] which has been interpreted in terms of intramolecular steric interactions.[17]

The solid state ^{31}P NMR features of **5** (Table 1) are similar to those of *cis*-$Pt(PHPh_2)_2(C_6F_5)_2$[3] and will not be commented further.

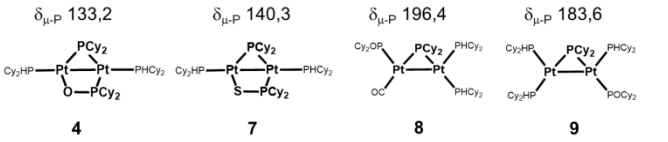

Chart III Bridging phosphanide ^{31}P resonances of molecules with a three membered Pt-μ-P-Pt ring with (**4**, **7**)or without (**8**, **9**) a fused four-membered ring.

Table 1 Experimental Solid-State and Solution ^{31}P Parameters of Complexes **3**, **4** and **5**.

Complex		ν_{rot}/(kHz)	δ_{11} (ppm)	δ_{22} (ppm)	δ_{33} (ppm)	δ_{iso} (ppm)[a]	$^{1}J_{P,Pt}$ (Hz)	Ω (ppm)[b]	κ[c]	$\delta_{solution}$ (ppm)
3	P^{1}	11.0	133(13)	65(9)	–625(10)	–142.6	2312	758	0.82	–137.9[d]
	P^{2}	11.0	97(1)	8(1)	–55(1)	16.9	1960	152	–0.17	15.1[d]
4	P^{1}	9.0				133.2	3096			134.4[e]
							3969			
	P^{2}	9.0				23.7	4278			15.9[e]
	P^{3}	9.0				97.3	3066			94.6[e]
	P^{4}	9.0				15.6	3668			18.5[e]
5		9.0	90(1)	–33(1)	–33(1)	7.8	3448	123	–1.00	3.6[f]
		9.0	95(1)	–43(1)	–65(1)	–4.9	3377	160	–0.73	3.6[f]

[a] Isotropic shift is defined as $\delta_{iso} = (\delta_{11} + \delta_{22} + \delta_{33})/3$; [b] $\Omega = \delta_{11} - \delta_{33}$; [c] $\kappa = 3(\delta_{22} - \delta_{iso})/\Omega$; [d] In $CDCl_3$, from ref. 11; [e] in C_6D_6, from ref. 11; [f] in $CDCl_3$, from ref. 18.

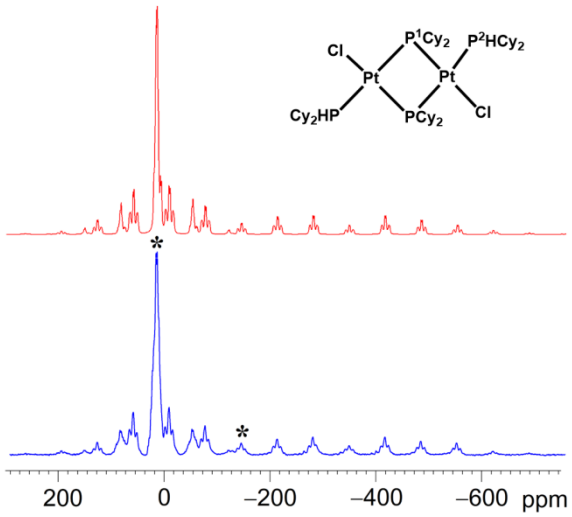

Fig. 2 ^{1}H-^{31}P CP/MAS spectrum of *anti*-[(PHCy$_2$)ClPt(μ-PCy$_2$)$_2$Pt[(PHCy$_2$)Cl], **3**, obtained with a MAS rate of 11.0 kHz, 6.0 s recycle delay (bottom trace) and spectral simulation using the data listed in Table 1 (top trace). The asterisks indicate the isotropic ^{31}P chemical shifts.

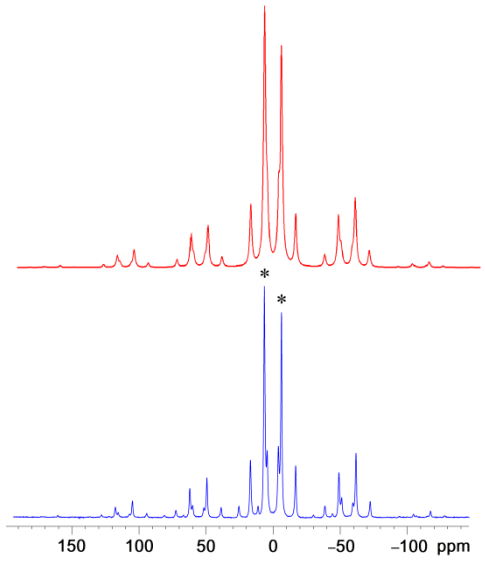

Fig. 4 ^{1}H-^{31}P CP/MAS spectrum of *cis*-PtCl$_2$(PHCy$_2$)$_2$, **5**, obtained with a MAS rate of 9.0 kHz (bottom trace) and spectral simulation using the data listed in Table 1 (top trace). The asterisks indicate the isotropic ^{31}P chemical shifts of the inequivalent P atoms.

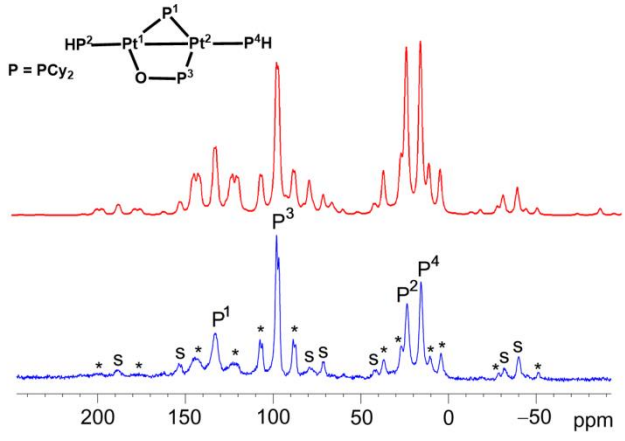

Fig. 3 ^{1}H-^{31}P CP/MAS spectrum of [(PHCy$_2$)Pt(μ-PCy*2*)(κ^2*P,O*-μ-POCy$_2$)Pt(PHCy$_2$)] (*Pt-Pt*), 4, obtained with a MAS rate of 9.0 kHz (bottom trace) and spectral simulation using the data listed in Table 1 (top trace); the asterisks denote ^{195}Pt satellites whereas "s" denotes spinning side bands.

^{1}H-^{195}Pt CP/CPMG NMR

Solid state ^{195}Pt NMR studies were performed using the method proposed by Wasylishen[19] and Schurko,[20] consisting in the application of the Carr-Purcell Meiboom-Gill (CPMG) pulse sequence.

The static ^{1}H-^{195}Pt CP/CPMG spectra of complexes **3**-**5** are shown in Figure 5. The isotropic chemical shift of the ^{195}Pt signal of **3** was found at δ –3970, in good agreement to the value found in solution (δ –4014).[11] The CSA of the ^{195}Pt signal of **3** is characterised by a span Ω of 4794 ppm and a skew of –0.52. These values are characteristic for a ^{195}Pt nucleus involved in a four-membered Pt$_2$P$_2$ ring. The span and skew values for the related complex **1** are: Ω = 4549 ppm; κ = –0.62.[3]

The ^{1}H-^{195}Pt CP/CPMG spectrum of complex **4** shows the overlapped pattern of the two different ^{195}Pt atoms. The attribution of δ_{11} and δ_{22} for each of the ^{195}Pt nuclei is straightforward, but the assignment of the distinct principal component δ_{33} to the proper ^{195}Pt nucleus is not unequivocal. However, since DFT calculations (*vide infra*) indicated that δ_{33} of Pt^1 fell at lower fields than δ_{33} of Pt^2, it was possible to assign the values of δ_{33} as –5850 ppm for Pt^1 and –5927 ppm for Pt^2. By using the principal component values collected in Table 2, the isotropic chemical shifts for the two ^{195}Pt atoms were calculated as δ_{Pt1} = –4833 and δ_{Pt2} = –5188.

Journal Name

ARTICLE

Table 2 Experimental Solid-State and Solution ^{195}Pt Parameters of **1**-**5**.

Complex		δ_{11} (ppm)	δ_{22} (ppm)	δ_{33} (ppm)	δ_{iso} (ppm)[a]	Ω (ppm)[b]	κ[c]	$\delta_{solution}$ (ppm)
1		–1023(48)	–4705(48)	–5954(48)	–3767(48)	4549(96)	–0.62(0.07)	–3795[d]
2		–4618(26)	–5594(26)	–5954(26)	–5389(26)	1337(52)	–0.46(0.04)	–5298[d]
3		–1160(26)	–4795(26)	–5954(26)	–3970(26)	4794(52)	–0.52(0.04))	–4014[e]
4	Pt^1	–4210(26)	–4440(26)	–5850(26)	–4833(26)	1640(52)	0.72(0.02)	–4796[f]
	Pt^2	–4658(26)	–4978(26)	–5927(26)	–5188(26)	1269(52)	0.50(0.02)	–5185[f]
5		–2180(26)	–5211(26)	–5981(26)	–4457(26)	3801(52)	–0.59(0.04)	–4540[e]

[a] Isotropic shift is defined as $\delta_{iso} = (\delta_{11} + \delta_{22} + \delta_{33})/3$; [b] $\Omega = \delta_{11} - \delta_{33}$; [c] $\kappa = 3(\delta_{22} - \delta_{iso})/\Omega$; [d] From ref. 3; [e] In $CDCl_3$, from ref. 11; [f] In C_6D_6, from ref. 11.

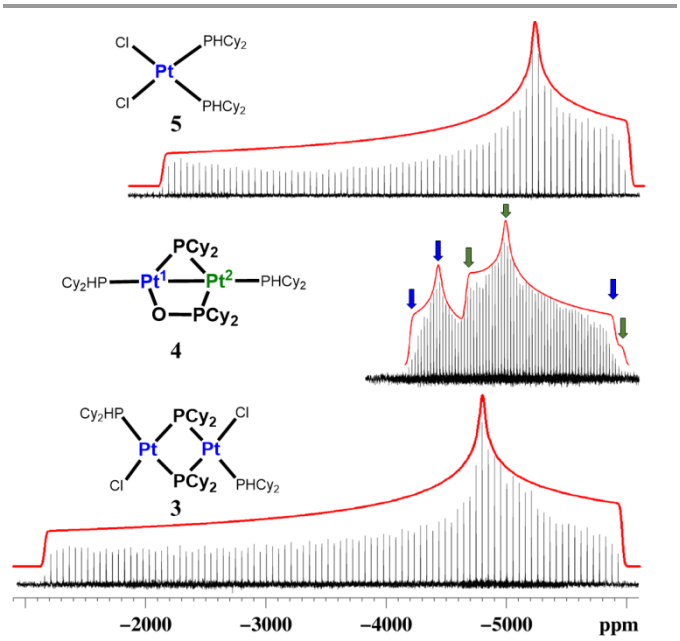

Fig. 5 Static ^{1}H-^{195}Pt CP/CPMG spectra (bottom trace) and simulations of powder patterns (top trace in red) of complexes **3**-**5**.

Such values are in good agreement to those found in C_6D_6 solution ($\delta_{Pt1} = -4796$; $\delta_{Pt2} = -5185$).[11]

The span of both ^{195}Pt nuclei of **4** (Ω = 1269 ppm for Pt^1, Ω = 1640 ppm for Pt^2) is much smaller compared to **3** (Ω = 4794 ppm). Such reduction of span can be attributed, *inter alia*, to the presence of the Pt–Pt bond as suggested by comparison with the span values of **1** (Ω = 4549 ppm, no Pt–Pt bond) and of **2** (Ω = 1337 ppm, presence of Pt–Pt bond).

The ^{1}H-^{195}Pt CP/CPMG spectrum of the mononuclear square planar complex **5** is characterised by a span Ω of 3801 ppm and a skew κ of –0.59. It is known that mononuclear square planar chloro-platinum complexes are characterised by very large CSA. For example, the CSA of K_2PtCl_4 is 10414 ppm[21] and the CSA of $PtCl_2N_2$ complexes (N = NH_3, pyridine, ½ ethylenediamine) ranges from 8325 to 9100 ppm.[22] The value found for **5** suggests that the presence of phosphorus atoms in place of nitrogen may provoke a strong reduction of the span.

DFT Calculation of ^{31}P and ^{195}Pt Chemical Shielding Tensor Parameters

The calculated principal components of the shielding tensor and isotropic value, and the corresponding chemical shifts, for the ^{195}Pt and ^{31}P nuclei in compounds **3** and **4** are reported in Table 3. For compound **3** the ^{31}P resonances are well reproduced in size and magnitude, though some disagreement is found for the bridging P^1. Also the principal components of the chemical shift tensor are in good agreement with the experimental results, see Table 3, with a non-negligible deviation only for the δ_{33} component. The agreement between calculated and experimental values is even better for the phosphane P^2. The same conclusion can be drawn for compound **4**. In Figure 6 the correlation graph between calculated and experimental ^{31}P chemical shifts is shown.

The calculated isotropic shielding constants of ^{195}Pt are also in good agreement with the experimental values, except for a systematic shift of about –500 ppm that might be also ascribed to the calculated reference ^{195}Pt shielding.

Thus the results of the calculations appears reliable and they would be quantitatively correct if one accounts for the systematic shift in passing from the shielding constants to the chemical shift scale. Based on these grounds we turned our attention to the principal components of the shielding tensors.

Journal Name

ARTICLE

Table 3 Calculated ^{195}Pt and ^{31}P Parameters of **3** and **4** (in ppm). Experimental values in (*italics*)

Complex		σ_{11}	σ_{22}	σ_{33}	σ_{iso}	δ_{11}	δ_{22}	δ_{33}	δ_{iso}
3	**Pt**	2752.4	5421.2	6568.95	4914.2	–1356.4	–4028.9	–5178.3	–3521.2 (*–3970*)
3	**P^1**	182.8	244.4	813.6	413.7	140.9 (*133*)	79.3 (*65*)	–489.9 (*–625*)	–90.0 (*–142.6*)
3	**P^2**	214.3	319.3	357.5	297	109.4 (*97*)	4.4 (*18*)	–33.8 (*–55*)	26.7 (*16.9*)
4	**Pt^1**	4951	5455.5	6593.2	5666.6	–3558.1	–4063.3	–5202.6	–4274.7 (*–4833*)
4	**Pt^2**	5079.2	5577.2	7075.3	5910.6	–3686.5	–4185.2	–5685.3	–4519.0 (*–5188*)
4	**P^1**	117.4	147.2	232.3	165.6	206.3	176.5	91.4	158.1 (*133.2*)
4	**P^2**	216.2	316.1	350	294.1	107.5	7.6	–26.3	29.6 (*23.7*)
4	**P^3**	150.2	206.4	252.3	202.9	173.5	117.3	71.4	120.8 (*97.3*)
4	**P^4**	192.5	320.5	335.9	283.0	131.2	3.2	–12.2	40.7 (*15.6*)

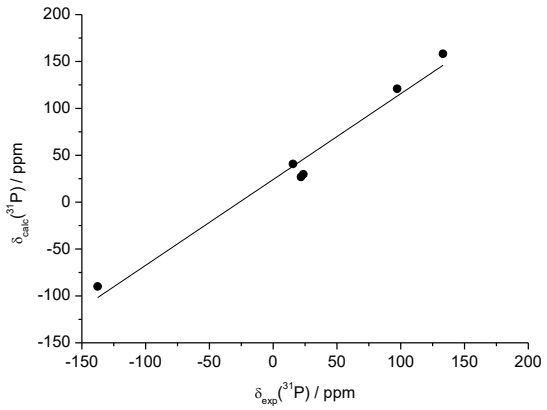

Fig. 6 Correlation between calculated and experimental ^{31}P chemical shifts. R^2 = 0.9693, $\delta_{calc} = a + b\,\delta_{exp}$: a = 24 ± 6 ppm, b = 0.92 ± 0.07.

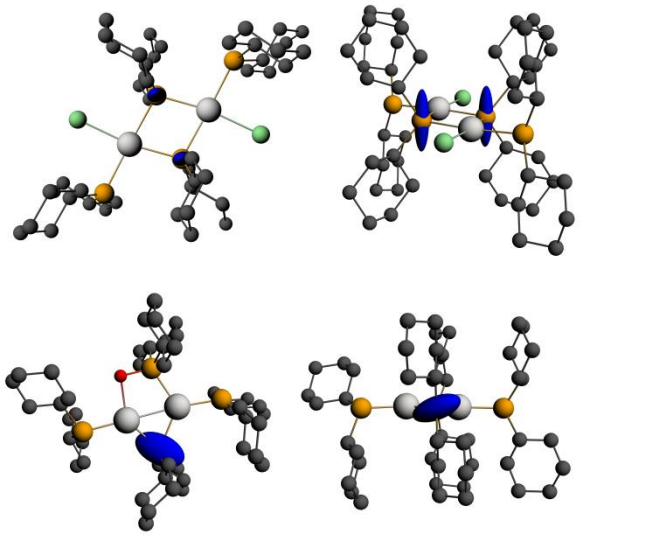

Fig. 7 Orientation of the shielding tensor of the ^{31}P nuclei of compound **3** (top) and **4** (bottom). Top view (left) and side view (right).

Examination of the orientation of the shielding tensor of the platinum atoms also reveals the components which are responsible for the difference in ^{195}Pt chemical shift between compounds **3** and **4**. Pt atoms in **4** are shielded by more than 1000 ppm with respect to **3**. As can be seen from Table 3 and Figure 8, it is, again, mostly the component perpendicular to the plane which, by increasing significantly, produces a general shielding of the Pt resonance. This increase is larger for Pt^2 which is, in fact, the most shielded Pt atom of **4**.

To summarise, both for ^{31}P and for ^{195}Pt resonances, the difference in chemical shift between **3** and **4** can be ascribed primarily to a change in the perpendicular component of their shielding tensors but in opposite directions: a decrease of the perpendicular component of the shielding tensor of P and an increase of the perpendicular component of shielding tensor of Pt.

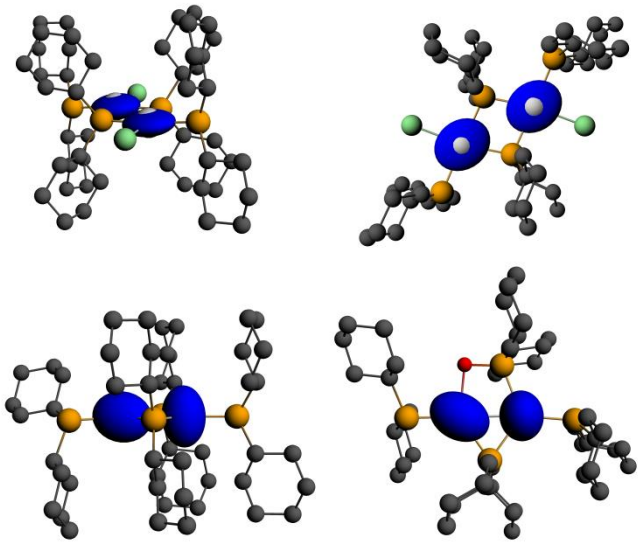

Fig. 8 Orientation of the shielding tensor of the ^{195}Pt nuclei of compound **3** (top) and **4** (bottom). Top view (left) and side view (right).

Finally, we analyzed the most important contribution to the isotropic shielding constant among the paramagnetic, diamagnetic and spin-orbit contributions. These are listed in Table 4 from which it is apparent that for ^{31}P the different values of σ_{iso} arise from differences in both σ_p and σ_{SO} while for ^{195}Pt the different values of σ_{iso} stem mainly from differences in σ_p, with a minor contribution from σ_{SO}. The diamagnetic contribution (σ_d) remains almost constant for ^{31}P and ^{195}Pt nuclei in both complexes.

Table 4 Calculated paramagnetic (σ_p), diamagnetic (σ_d) and spin-orbit (σ_{SO}) contribution to the ^{195}Pt and ^{31}P isotropic shielding constants.

Complex		σ_p	σ_d	σ_{SO}	σ_{tot}
3	Pt	–6918.3	9282.0	2550.5	4914.2
3	P^1	–651.8	956.4	109.1	413.7
3	P^2	–673.5	956.0	14.7	297
4	Pt^1	–6388.7	9279.6	2775.7	5666.6
4	Pt^2	–6177.1	9282.2	2805.5	5910.6
4	P^1	–775.5	956.0	–14.7	165.6
4	P^2	–670.1	956.6	7.6	294.1
4	P^3	–779.4	954.8	27.5	202.9
4	P^4	–689.3	955.9	16.2	283.0

Experimental

Complexes **3**,[11] **4**,[13] and **5**[18] were prepared by literature methods.

Solid-State NMR

Solid-state NMR experiments were performed on a Bruker Avance I 400 spectrometer using a 4.0 mm HX MAS probe at 298 K. For MAS and static (non-spinning) experiments, samples were packed in zirconia rotors. Chemical shifts are referenced to H_2PtCl_6 (^{195}Pt, 86.0 MHz) and H_3PO_4 (^{31}P, 161.9 MHz). For ^{31}P and ^{195}Pt NMR spectra, a two-pulse phase-modulation (TPPM) decoupling scheme was used for the ^{1}H decoupling.

^{1}H-^{31}P CP/MAS NMR experiments were performed using 3.25 μs proton $\pi/2$ pulse length, ν_{CP} of 55.0 kHz, contact time of 5.0 ms, $\nu_{\delta ec}$ of 76.9 kHz and recycle delay of 6 s. ^{1}H-^{31}P CP/MAS NMR spectrum of complex **3** was acquired collecting four subspectra using spectral width of 65.0 kHz. The transmitter offset was set at 58311 Hz, –6479 Hz, –71269 Hz and –136069 Hz. ^{1}H-^{31}P CP/MAS NMR spectra of complexes **4** and **5** were acquired using spectral width of 65.0 kHz with the a transmitter offset set at 0 Hz. The line width at half height of the peaks are 800 Hz for **3** and 180 Hz for **5**, while ranged from 270 Hz to 600 for **4**.

Static solid state ^{195}Pt NMR spectra were acquired using the Cross-Polarization-Carr-Purcell Meiboom-Gill (CP-CPMG) pulse sequence.[19-20] ^{195}Pt powder patterns were obtained by collecting subspectra with a spectral width of 75 kHz and 50 Meiboom-Gill (MG) loops. For complex **3**, twelve subspectra were acquired using transmitter offsets spaced by 26.6 KHz (the first transmitter offset was set at –514456 Hz), for complex **4** ten subspectra spaced by 13.3 KHz (the first transmitter offset was set at –498887 Hz), and for complex **5** twelve subspectra spaced by 26.6 KHz (the first transmitter offset was set at –487876 Hz). In all cases, the subspectra were co-added using the skyline projection method. The acquisition time ($1/\tau_a$) was adjusted to attain a spikelet separation of 4.4 kHz for all three complexes. The ^{195}Pt spectra were performed using 3.25 μs proton $\pi/2$ pulse length, ν_{CP} of 65.4 kHz, contact time of 7.0 ms, ν_{dec} of 77.0 kHz, and recycle delay of 4 s. The spinning rates for ^{1}H-^{31}P CP/MAS NMR spectra were chosen in such a way that the second-order effects were completely averaged.[24] The ^{1}H-^{31}P CP/MAS NMR spectrum of **3** was recorded at various spinning rates in search of conditions that minimized spinning sideband overlapping. The spectrum recorded at 11.0 kHz spinning rate was used for Herzfeld-Berger (HB) analysis of the ^{31}P phosphanido signal.

For **4** and **5** the ^{1}H-^{31}P CP/MAS NMR spectra were acquired at 9 KHz. Simulations of static spectra were carried out with WSOLIDS,[25] while simulation of MAS spectra was carried out with SIMPSON.[26] The shown calculated solid-state ^{31}P NMR spectra were obtained as addition of three subspectra of isotopomers having no (natural abundance: 43.8%), one (natural abundance: 44.8%) or two (natural abundance: 11.4%) NMR active ^{195}Pt atoms. The principal components of the ^{31}P chemical shift tensors were obtained from Herzfeld-Berger (HB) analysis of the sideband patterns[27] by using the program Graphical Herzfeld Berger Analysis.[28]

Computational Details

Geometries were minimized using the BP86 functional[29] with the triple-ζ, polarized basis set TZ2P. The correction for dispersive interactions by Grimme, DFT-D3,[30] was included. NMR properties of ^{195}Pt and ^{31}P nuclei were calculated with the ADF NMR module[31] from the ZSO density and yielded the full shielding tensor and its principal components σ_{11}, σ_{22}, and σ_{33}, with $\sigma_{33} \geq \sigma_{22} \geq \sigma_{11}$. Chemical shifts were determined as $\delta_{ii} = (\sigma_{ref} - \sigma_{ii})/(1 - \sigma_{ref})$ using the commonly adopted reference

$[PtCl_6]^{2-}$ (σ_{ref} = 1397.9 ppm)[32] for ^{195}Pt and as $\delta_{ii} = (\sigma_{ref} - \sigma_{ii} - 266.1)$[33] relative to 85% H_3PO_4 using the magnetic shielding constant of PH_3 (σ_{ref} = 589.8 ppm) calculated at the same computational level as the secondary reference. For the NMR calculations a mixed basis set: TZ2P for Pt, P, Cl and O atoms while the TZP basis set was used for the C and H atoms in order to reduce the computational demand. All calculations were run with the Amsterdam Density-Functional (ADF 2013) package, using the keyword zsoao2007 in the NMR module as a workaround to remove a known bug of ADF version 2013.[34]

Conflicts of interest

There are no conflicts to declare.

Conclusions

In conclusion, isotropic ^{195}Pt (and ^{31}P) chemical shifts of diorganophosphanido platinum complexes are dependent on the geometrical features of the molecule (a major role being played by the presence or absence of a Pt–Pt bond subtended by the μ-P) rather than on the formal oxidation state of the platinum.[23]

Analysis of the solid state ^{31}P NMR features of the phosphanido Pt complexes **1**,[3] **3** and **6**[12] indicates that the four-membered Pt_2P_2 ring is endowed with a high value of the span (> 700 ppm) and a positive (close to 1.0) value of the skew, independently from the substituent on P and Pt. Comparing complexes **4** and **7** with **8** and **9** suggests that the presence of a four-membered ring (**4** or **7**) fused with the three-membered Pt_2P ring (**8** and **9**) may cause a reduction of the μ-P[1] span, resulting in significantly lower values of ^{31}P isotropic chemical shifts ($\Delta\delta \approx 50$ ppm). The ^{195}Pt NMR features of complexes **3** and **4** showed a strong reduction of the Ω span on going from **3** to **4**; an effect imputable to only one of the three components of the CS tensor. Relativistic DFT calcultions revealed that, as already found for **1** and **2**,[3] the largest component of the shielding tensor for the μ-P as well as for the Pt atoms is oriented perpendicularly to the coordination plane of the complex and that different values of the isotropic shieldings between **3** and **4** originate from differences in the paramagnetic and spin-orbit contributions.

Acknowledgements

Calculations were run on the Linux cluster of the C3P consortium of the Department of Chemical Sciences of the University of Padova.

Notes and references

1 D. C. Apperley, R. K. Harris, P. Hodgkinson. *Solid State NMR: Basic Principles and Practice*. Momentum Press LLC: New York, 2012.

2 a) P. Mastrorilli, *Eur. J. Inorg. Chem.*, 2008, **31**, 4835-4850; b) C. Fortuño, A. Martín, P. Mastrorilli, V. Gallo, S. Todisco *Organometallics*, 2017, **36**, 4325-4337; c) D. Giardina-Papa, I. Ara, S. Ibáñez, P. Mastrorilli, V. Gallo, J. Fornies, *Polyhedron*,2016, **120**, 44-53; d) P. Mastrorilli, V. Gallo, S. Todisco, M. Latronico, G. Saielli, *Chem. Eur. J.*, 2016, **22**, 7964-7969; e) I. Ara, J. Forniés, S. Ibáñez, P. Mastrorilli, S. Todisco, V. Gallo, *Dalton Trans.*, 2016, **45**, 2156-2171; f) M. Latronico, P. Mastrorilli, V. Gallo, S. Todisco, M. M. Dell'Anna, A. Rizzuti, *Eur. J. Inorg. Chem.*, 2015, **15**, 2579-2586; g) Mario Latronico, Vito Gallo, Elena Lalinde, Santiago Ruiz, Stefano Todisco, Piero Mastrorilli, *Inorganics*, 2014, **2**, 591-605; h) A. Arias, J. Fornies, C. Fortuño, A. Martín, P. Mastrorilli, V. Gallo, S. Todisco, *Eur. J. Inorg. Chem.*, 2014, **10**, 1679-1693; i) M. Latronico, S. Todisco, V. Gallo, U. Englert, P. Mastrorilli, Eur. J. *Inorg. Chem.*, 2014, **10**, 1669-1678; j) A. Arias, J. Fornies, C. Fortuño, S. Ibanez, A. Martín, P. Mastrorilli, V. Gallo, S. Todisco, *Inorg. Chem.*, 2013, **52**, 11398-11408; k) A. Arias, J. Fornies, C. Fortuño, A. Martín, P. Mastrorilli, S. Todisco, M. Latronico, V. Gallo, *Inorg. Chem.*, 2013, **52**, 5493-5506; l) J. Fornies, C. Fortuño, S. Ibanez, A. Martín, P. Mastrorilli, V. Gallo, A. Tsipis, *Inorg. Chem.*, 2013, **52**, 1942-1953; m) M. Latronico, S. Sanchez, A. Rizzuti, V. Gallo, F. Polini, E. Lalinde, P. Mastrorilli *Dalton Trans.*, 2013, **42**, 2502-2511; n) A. Arias, J. Fornies, C. Fortuño, A. Martín, M. Latronico, P. Mastrorilli, S. Todisco, V. Gallo, *Inorg. Chem.*, 2012, **51**, 12682-12696; o) J. Forniés, C. Fortuño, S. Ibáñez, A. Martín, P. Mastrorilli, V. Gallo, *Inorg. Chem.*, 2011, **50**, 10798-10809; p) M. Latronico, P. Mastrorilli, V. Gallo, M. M. Dell'Anna, F. Creati, N. Re, U. Englert, *Inorg. Chem.*, 2011, **50**, 3539-3558; q) J. Forniés, C. Fortuño, S. Ibáñez, A. Martín, P. Romero, P. Mastrorilli, V. Gallo, *Inorg. Chem.*, 2011, **50**, 285-298; r) P. Mastrorilli, M. Latronico, V. Gallo, F. Polini, N. Re, A. Marrone, R. Gobetto, S. Ellena, *J. Am. Chem. Soc.*, 2010, **132**, 4752-4765; s) I. Ara, J. Forniés, C. Fortuño, S. Ibáñez, Antonio Martín, P. Mastrorilli, V. Gallo, *Inorg. Chem.*, 2008, **47**, 9069-9080; t) P. Mastrorilli, *Dalton Trans.*, 2008, 4555-4557.

3 P. Mastrorilli, S. Todisco, A. Bagno, V. Gallo, M. Latronico, C. Fortuño, D. Gudat, *Inorg. Chem.*, 2015, **54**, 5855–5863.

4 M. Kaupp, O. L. Malkina, V. G. Malkin, P. Pyykko, *Chem. Eur. J.*, 1998, **4**, 118-126.

5 G. Casella, A. Bagno, S. Komorovsky, M. Repisky, G. Saielli, *Chem. Eur. J.*, 2015, **21**, 18834-18840.

6 G. Saielli, A. Bagno, F. Castiglione, R. Simonutti, M. Mauri, A. Mele, *J. Phys. Chem. B*, 2014, **118**, 13963–13968.

7 A. Bagno, G. Saielli, *Chem. Eur. J.*, 2012, **18**, 7341-7345.

8 L. A. Truflandier, E. Brendler, J. Wagler, J. Autschbach, *Angew. Chem. Int. Ed.*, 2011, **50**, 255-259.

9 K. P. Kornecki, J. F. Briones, V. Boyarskikh, F. Fullilove, J. Autschbach, K. E. Schrote, K. M. Lancaster, H. M. L. Davies, J. F. Berry, *Science*, 2013, **342**, 351-354

10 a) F. Alkana, C. Dybowski, *Phys. Chem. Chem. Phys.*, 2015, **17**, 25014-25026; b) F. Alkana, C. Dybowski, *Phys. Chem. Chem. Phys.*, 2014, **16**, 14298-14308.

11 V. Gallo, M. Latronico, P. Mastrorilli, C. F.Nobile, G. P. Suranna, G. Ciccarella, U. Englert, *Eur. J. Inorg. Chem.*, 2005, **22**, 4607-4616.

12 I. V. Kourkine, M. B. Chapman, D. S. Glueck, K. Eichele, R. E. Wasylishen, G. Y. A. Yap, L. M. Liable-Sands, A. L. Rheingold, *Inorg. Chem.*, 1996, **35**, 1478-1485.

13 V. Gallo, M. Latronico, P. Mastrorilli, C. F. Nobile, F. Polini, N. Re, U. Englert, *Inorg.Chem.*, 2008, **47**, 4785-4795.

14 L. Bemi, H. C. Clark, J. A. Davies, C. A. Fyfe, R. E. Wasylischen, *J. Am. Chem. Soc.*, 1982, **104**, 438-445.

15 J. H. Nelson, J. A. Rahn, W. A. Bearden, *Inorg. Chem.*, 1987, **26**, 2192-2193.

16 J. A. Rahn, L. Baltusis, J. H. Nelson, *Inorg. Chem.*, 1989, **28**, 2631-2635.

17 J. A. Rahn, D. J. O'Donnell, A. R. Palmer, J. H. Nelson, *Inorg. Chem.*, 1990, **29**, 750-755.

18 P. Mastrorilli, C. F. Nobile, F. P. Fanizzi, M. Latronico, C. Hu, U. Englert, *Eur. J. Inorg. Chem.* 2002, 1210-1218.

19 R. Siegel, T. T. Nakashima, R. E. Wasylishen, *J. Phys. Chem. B*, 2004, **108**, 2218-2226.
20 I. Hung, A. J. Rossini, R. W. Schurko, *J. Phys. Chem. A*, 2004, **108**, 7112-7120.
21 S. W. Sparks, P. D. Ellis, *J. Am. Chem. Soc.*, 1986, **108**, 3215-3218.
22 B. E. G. Lucier, A. R. Reidel, R. W. Schurko, *Can. J. Chem.*, 2011, **89**, 919-937.
23 a) J. R. L. Priqueler, I. S. Butler, F. D. Rochon, *Appl. Spectrosc. Rev.*, 2006, 41, 185-226; b) B. M. Still, P. G. A. Kumar, J. R. Aldrich-Wright, W. S. Price, *Chem. Soc. Rev.*, 2007, **36**, 665-686.
24 R. Challoner, A. Sebald, *Solid State Nucl. Magn. Reson.*, 1995, **4**, 39-45.
25 K.Eichele, R. E. Wasylishen, *WSolids1 ver. 1.20.21*, Universität Tübingen, 2013.
26 M. Bak, J. T. Rasmussen, N. C. Nielsen, *J. Magn. Reson.*, 2000, **147**, 296-330.
27 J. Herzfeld, A. E. Berger, *J. Chem. Phys.*, 1980, **73**, 6021-6030.
28 K. Eichele, *HBA 1.7*, Universität Tübingen, 2012.
29 a) A. D. Becke *Phys. Rev. A*, 1988, **38**, 3098-3100; b) J. P. Perdew *Phys. Rev. B*, 1986, **33**, 8822-8824; c) J. P. Perdew *Phys. Rev. B*, 1986, **34**, 7406-7406.
30 G. te Velde, F. M. Bickelhaupt, E. J. Baerends, C. Fonseca Guerra, S. J. A. van Gisbergen, J. G. Snijders, and T. Ziegler *J. Comput. Chem.*, 2001, **22**, 931-967.
31 a) G. Schreckenbach, T. Ziegler, *J. Phys. Chem.*, 1995, **99**, 606-611; b) S. K. Wolff, T. Ziegler, *J. Chem. Phys.*, 1998, **109**, 895-905.; c) G. Schreckenbach, T. Ziegler, *Int. J. Quantum Chem.*, 1997, **61**, 899-918.; d) S. K. Wolff, T. Ziegler, E. van Lenthe, E. J. Baerends, *J. Chem. Phys.*, 1999, **110**, 7689-7698.
32 A. Bagno, R. Bini, *Angew. Chem. Int. Ed.*, 2010, **49**, 1083-1086.
33 C. van Wüllen, *Phys. Chem. Chem. Phys.*, 2000, **2**, 2137-2144.
34 S. Moncho, J. Autschbach, *J. Chem. Theory Comput.*, 2010, **6**, 223-234.